DETERMINING ICEBERG SCATTERING MECHANISMS IN GREENLAND USING QUAD POL ALOS-2 SAR DATA

Johnson Bailey[1] Armando Marino[1] Vahid Akbari[1]

[1]The University of Stirling, Faculty of Natural Sciences, Stirling, UK

ABSTRACT

Iceberg properties, together with meteorological and environmental conditions can influence Synthetic Aperture Radar (SAR) backscatter behaviours. In this work, we used five images of quad-pol ALOS-2/PALSAR-2 SAR data to analyse icebergs in Greenland. We investigate the scattering mechanisms through several observables and decompositions. Our results show that the most common scattering mechanisms for icebergs is surface scattering and volume scattering. Sometimes double bounce is also observed. By performing a multi-scale analysis using boxcar 5 × 5 and 11 × 11 window sizes, we conclude that icebergs can be a collection of strong scatterers. This gives hope for using quad-pol polarimetry to provide some iceberg classifications in the future.

Index Terms— SAR, polarimetry, icebergs, backscatter

1. INTRODUCTION

The aim of this paper is to analyse the scattering mechanisms of icebergs based on a series of polarimetric parameters, which include the Cloude–Pottier decomposition [1], the Yamaguchi decomposition, Pauli RGB and backscatter intensity (span). Polarimetric behaviour is compared by performing a multi-scale analysis using two boxcar 5 x 5 and 11 x 11 window sizes.

The scattering matrix [2], characterises the polarimetric backscattering property of a target.

$$S = \begin{bmatrix} HH & HV \\ VH & VV \end{bmatrix} \tag{1}$$

H stands for linear-horizontal polarisation and V for linear-vertical polarisation. The transmission of a linear vertical wave, which is then received as a linear horizontal wave, gives HV. We can also use a scattering vector $\underline{k}$ to characterise a polarised target:

$$\underline{k} = \frac{1}{2}Trace([S]\psi) = [k_1, k_2, k_3, k_4]^T \tag{2}$$

where *Trace* refers to the sum of all diagonal elements of a matrix and ψ is a basis for a 2 × 2 Hermitian matrix. k_1, k_2 and k_3 are complex numbers. In the case of a monostatic sensor or a reciprocal medium, HV = VH, except for noise and $\underline{k}$, becomes a three-dimensional complex. We define scattering mechanism or projections vector as a normalised $\underline{k}$ vector [3].

$$\underline{\omega} = \frac{\underline{k}}{|\underline{k}|} \tag{3}$$

Acquiring the full scattering matrix provides quad-polarimetric (quad-pol) data. Sometimes, it is the case that pixels contain different polarimetric behaviours. The scattering matrix alone cannot characterise these. We therefore produce a 3 x 3 covariance matrix to extract the second order statistics:

$$C = \langle \underline{k} \cdot \underline{k}^{*T} \rangle = \begin{bmatrix} \langle |k_1|^2 \rangle & \langle k_1 k_2^* \rangle & \langle k_1 k_3^* \rangle \\ \langle k_2 k_1^* \rangle & \langle |k_2|^2 \rangle & \langle k_2 k_3^* \rangle \\ \langle k_3 k_1^* \rangle & \langle k_3 k_2^* \rangle & \langle |k_3|^2 \rangle \end{bmatrix} \tag{4}$$

where <> is an averaging operator, * is a complex conjugate and T is the matrix transpose.

2. MATERIALS AND METHODS

Each SAR image was taken from the PALSAR-2 instrument aboard the ALOS-2 radar satellite over Greenland. These data were collected under an open JAXA Announcement of Opportunity. A total of five images were selected for analysis, processed via calibration, construction of a covariance matrix, boxcar filtering and finally, PolSAR parameters. We then performed a multi-scale analysis using two window sizes. A description of the SAR data is presented in Table 1.

Table 1. ALOS-2/PALSAR-2 JAXA properties. Note the ground resolution is for ALOS-2/PALSAR-2 quad-pol mode. Time is UTC.

Image ID	Location	Resolution	Date/Time
ALOS2066231360-150815	Blosseville Coast N	4.3×5.1	15/08/2015 01:26
ALOS2064761430-150805	Nuugaatsiaq	4.3×5.1	05/08/2015 02:48
ALOS2064461300-150803	Isortoq	4.3×5.1	03/08/2015 02:07
ALOS2057951350-150620	Blosseville Coast S	4.3×5.1	20/06/2015 01:26
ALOS2191031530-171206	Savissivik	4.3×5.1	06/12/2017 02:52

We calibrated ALOS-2 quad-pol data into the appropriate SAR real and imaginary parts for each image. Next, we produced the covariance matrices to extract second order statistics. We used two filters either of 5×5 (which corresponds to 25.5×21.5 m) or 11×11 (which corresponds to 56.1×47.3 m) to apply averaging. After the filtering, the data (in covariance matrix format) are ready to be processed for extracting decomposition parameters (Cloude–Pottier, Yamaguchi) or other observables (Pauli RGB and span).

To visualise the icebergs, we used the RGB images with large zooms (500×500 pixels) and adjusted contrast. The RGB images were composed with the intensities of the Pauli components: HH + VV for red, HH-VV for green and 2 HV for blue. Other targets such as ships and charter rocks were eliminated from the analysis. Each iceberg was identified via the middle pixel in radar coordinates.

Since we are missing in situ validation data, our analysis is restricted to icebergs we can identify visually. Because backscattering behaviour may be dependent on environmental factors such as the presence of surface liquid water, we collated meteorological data for the nearest available weather stations. There is more information in [4] but Table 2 outlines the meteorological data record.

Table 2. Average Greenland meteorological conditions for images taken. Each location is a weather observation station.

Location	Min Temperature (°C)	Average Rainfall (mm)	Average Wind Speed (km/h)	Date Taken
Angmagssalik	−3	5.44	6.9	03/08/2015
Angmagssalik	−4	25.18	7.6	20/06/2015
Angmagssalik	−3	5.44	6.9	15/08/2015
Qaarsut Airport	1	78.94	6.2	05/08/2015
Thule Air Base	−18	4.83	11.7	06/12/2017

3. RESULTS

Here, we show the main results of the analysis. A more detailed description of the results is available in [4].

We first analyse the target entropy, a parameter derived from the Cloude-Pottier decomposition. Here, it is an indicator of the presence of dominant scatterers or the closeness of the backscattering to the noise floor (which will increase the value of entropy). The alpha angle is obtained from the 3 eigenvalues of the covariance matrix and is used to determine the type of scattering mechanism present (odd bounce, even bounce or dipoles). The span is the total intensity of the RGB channels and determines the value of backscatter from the icebergs. Figure 1 shows the alpha entropy plot and Figure 2 shows the entropy span plot.

We also show results from the analysis using the four component Yamaguchi decomposition. The four scattering mechanisms analysed are double bounce, surface, volume and helix scattering. Here the algorithm avoids instability by clipping low values to the lowest value in the image. This is the reason for repeated lowest values in the plots. Figures 3, and 4 show the model results.

4. DISCUSSION

We note large entropy values in the icebergs. We also performed a multi-scale analysis to check if icebergs can be approximated as (a) partial targets (b) single targets or (c) a mixture of single targets. Looking at the differences in entropy, when the window was changed from 5×5 to 11×11, we conclude that icebergs are a combination of all three and therefore, entropy cannot be used on its own to detect icebergs. That there is no significant effect on the entropy from temperature change may be attributed to a negligent amount of surface liquid water.

4.1. Target Characteristics

The total backscattering varies greatly going down to values around −28 dB. This is especially visible in Isortoq, where icebergs were visible for a short time, floating in an area with low ocean backscatter. This corroborates the fact that backscattering signals from open water may be stronger than backscatter signals from smaller icebergs [5]. Besides Isortoq, most of the icebergs are above −10 dB, showing a relatively strong signal. These higher signals suggest smoother icebergs, and less volume scattering, which is supported by Viehoff [6].

When the entropy goes higher, this forces the average alpha to increase towards 60°. If there is a dominant mechanism in an iceberg, this seems to be a mix of surface or dipole scattering. However, in a few icebergs there is a dominant double bounce contribution, although it is rare overall. The values for the 5×5 window are mostly spread. Estimating anisotropy requires a large average. The alpha angle varies significantly for different icebergs going mostly from surface to dipoles. This suggests that icebergs can appear in images with a polarimetric behaviour which will resemble mostly a surface or volume scattering.

4.2. Model Based Analysis

In the volume vs. surface plot (Figure 4) when the backscattering signal is high, surface scattering seems to be dominant. An increased penetration might lower the backscatter signal and increase volume scattering, indicating an increased loss in the iceberg body and the presence of features in the ice body [7],[8]. In the surface vs. double bounce plot (Figure 3), surface scattering is again dominant in most of the icebergs with 5×5, except a few exceptions where the double bounce is stronger. Double bounce seems to be dominant only in a limited number of icebergs. However, when we compare double bounce to volume, we show that the latter seems to be stronger in most cases. Our findings suggest icebergs tend to have either surface or volume scattering, or a combination between surface and multiple reflections.

Finally, regarding eventual effects of surface liquid water, observing the volume vs. surface plot (Figure 4) for Blosseville Coast N and S, colder conditions reduce the scattering, corroborating with an increased penetration within the ice body.

5. CONCLUSION

This analysis found that icebergs exhibit a combination of surface and volume scattering, in all conditions. In some rarer instances, double bounce dominates the scattering. We
show that analysing just the entropy will not be sufficient for iceberg classification from SAR imagery. We found differences in scattering behaviour between icebergs in similar locations but at different times of the year. The analysis shows that polarimetry at L-band has potential for classifying iceberg geometry and presence of liquid water. However, classification requires in situ validation dataset which is currently not available.

We suggest a further comparative analysis showing more iceberg locations and times of the year in the Arctic. Additionally, investigating the link between shape of icebergs and applying PolSAR scattering models developed for glaciers.

6. ACKNOWLEDGEMENTS

7. REFERENCES

[1]   S. R. Cloude and E. Pottier, "A review of target decomposition theorems in radar polarimetry," *IEEE transactions on geoscience and remote sensing,* vol. 34, no. 2, pp. 498-518, 1996.

[2]   G. Sinclair, "The transmission and reception of elliptically polarized waves," *Proceedings of the IRE,* vol. 38, no. 2, pp. 148-151, 1950.

[3]   S. Cloude, *Polarisation: applications in remote sensing*. Oxford university press, 2010.

[4]   J. Bailey and A. Marino, "Quad-Polarimetric Multi-Scale Analysis of Icebergs in ALOS-2 SAR Data: A Comparison between Icebergs in West and East Greenland," *Remote Sensing,* vol. 12, no. 11, p. 1864, 2020.

[5]   C. Wesche and W. Dierking, "Iceberg signatures and detection in SAR images in two test regions of the Weddell Sea, Antarctica," *Journal of Glaciology,* vol. 58, no. 208, pp. 325-339, 2012.

[6]   T. Viehoff and A. Li, "Iceberg observations and estimation of submarine ridges in the western Weddell Sea," *International Journal of Remote Sensing,* vol. 16, no. 17, pp. 3391-3408, 1995.

[7]   J. D. Kirkham *et al.*, "Drift-dependent changes in iceberg size-frequency distributions," *Scientific reports,* vol. 7, no. 1, pp. 1-10, 2017.

[8]   C. Willis, J. Macklin, K. Partington, K. Teleki, W. Rees, and R. Williams, "Iceberg detection using ERS-1 synthetic aperture radar," *International Journal of Remote Sensing,* vol. 17, no. 9, pp. 1777-1795, 1996.
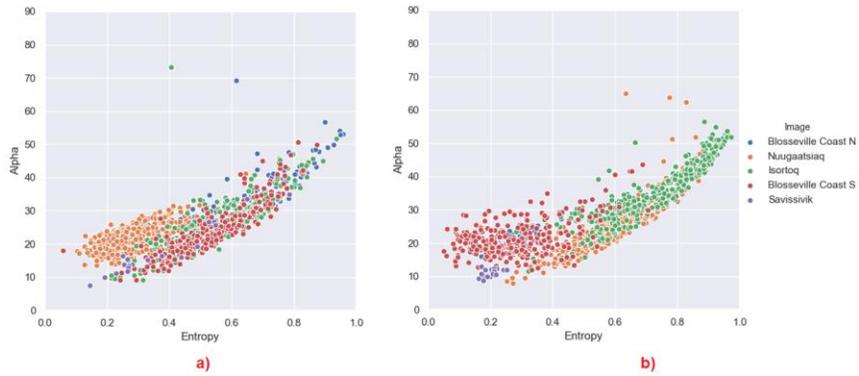
Figure 1. (a) Iceberg alpha, entropy plot 5 × 5 window, **(b)** 11 × 11 window. Entropy is between 0 and 1. Alpha is between 0 and 90. Colour legend indicates image. Dots indicate icebergs.
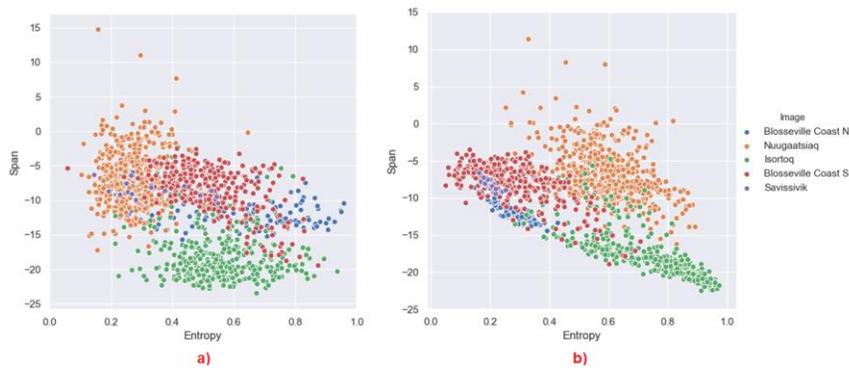
Figure 2. (a) Iceberg entropy, span plot 5x5 window **(b)** 11x11 window. Note the negative values for span. Entropy values are between 0 and 1. Colour legend indicates each image, each dot is an iceberg.
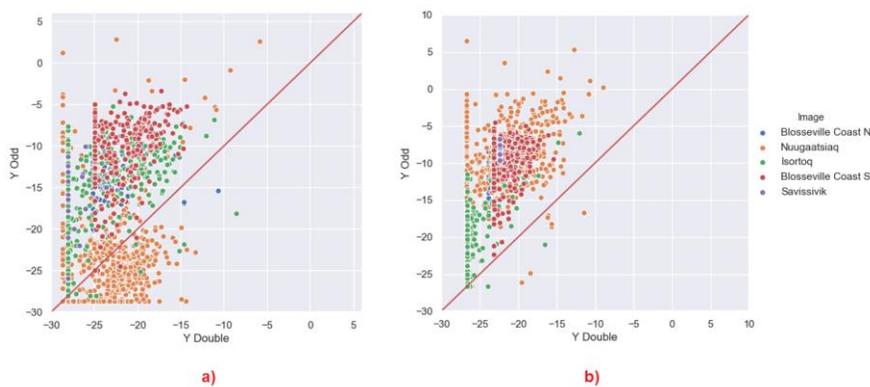
Figure 3. (a) Iceberg double bounce scattering, surface scattering plot in a 5 × 5 window, **(b)** 11 × 11 window. The majority of icebergs show surface scattering. Colour legend indicates image. Dots indicate icebergs. All values are in dB.
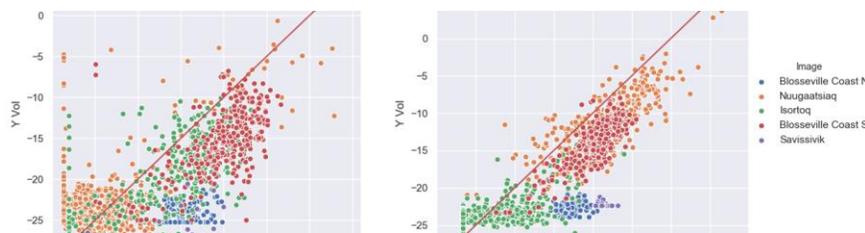
Figure 4. (a) Iceberg volume scattering, surface scattering plot in a 5 × 5 window, **(b)** 11 × 11 window. The majority of icebergs show volume scattering. Colour legend indicates image. Dots indicate icebergs. All values are in dB.